Supplement to manuscript:
Feedback mechanisms controlling Antarctic glacial cycle dynamics simulated with a coupled ice sheet–solid Earth model

Torsten Albrecht [1], Meike Bagge [2], and Volker Klemann [2]

[1]Potsdam Institute for Climate Impact Research (PIK), Member of the Leibniz Association, Potsdam, Germany
[2]GFZ German Research Centre for Geosciences, Telegrafenberg, 14473 Potsdam, Germany

Correspondence: T. Albrecht (albrecht@pik-potsdam.de)

In this supplement, we present further material. It is used in the manuscript to stress the discussed results. In addition (p. 6ff.), we show the impact of further 3D structures, which are based on the investigation of Bagge et al. (2021) and which highlights the sensitivity of Antarctic Ice Sheet response to spatial variability in 3D Earth structures.

List of supplementary figures

List of supplementary videos

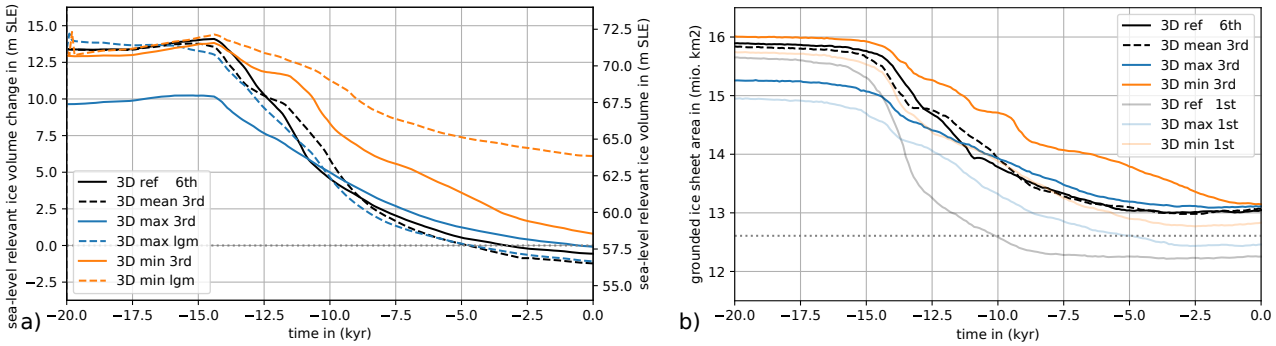

Figure S 1. Sea-level relevant Antarctic ice volume and grounded ice area over last 20 kyr for different Earth structure configurations. a) Sea-level relevant Antarctic ice volume in last iteration for '3D ref', '3D max' and '3D min' as well as the ice sheet's response for '3D max' and '3D min', when spun-up with the ice volume history of the '3D ref' case until 20 kyr BP ('lgm'). Black dashed is the ice sheet response for '3D mean'. b) Grounded ice area in three cases, with transparent lines for first iteration. Dotted horizontal line is present-day observation from Bedmap2 (Fretwell et al., 2013).

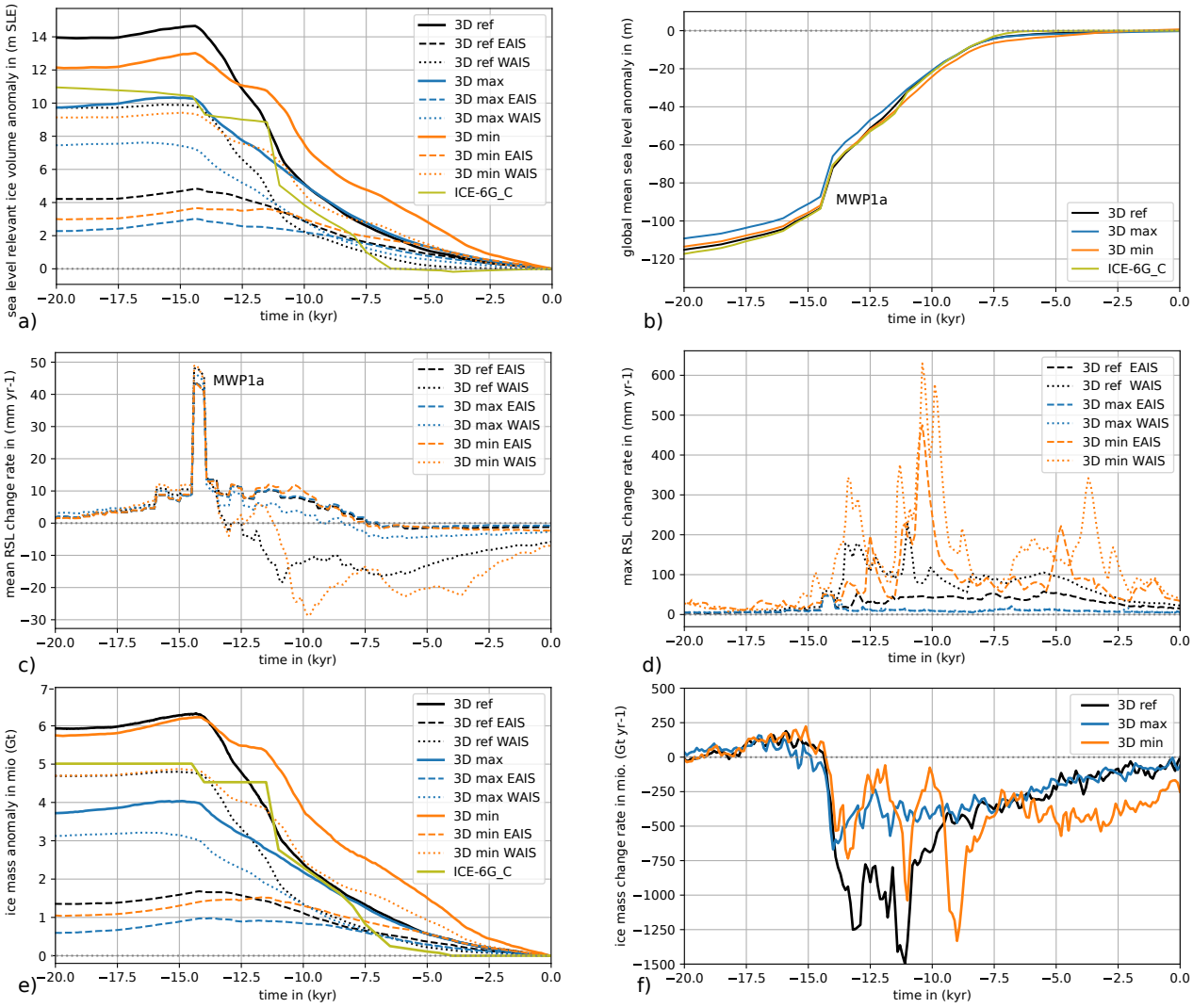

Figure S 2. Antarctic ice volume and change in relative sea level over last 20 kyr for different Earth structures. a) Anomaly in sea-level relevant Antarctic ice volume, b) global mean change in relative sea level (RSL), c) mean change rates of RSL, d) maximum change rates of RSL, e) anomaly in Antarctic ice mass and f) change rates in Antarctic ice mass with 100 yr resolution. Blue and orange lines show the response of the ice sheet to '3D max' and '3D min' Earth structure, respectively, black indicates the ice sheet response to '3D ref'. Dashed lines show the response for East Antarctica (75% of the ice-covered area), dotted for West Antarctica (25%), and (on the left) solid lines the sum of both. Olive lines show the reconstructions from ICE-6G_C. Melt water pulse 1A is indicated as 'MWP1a'.

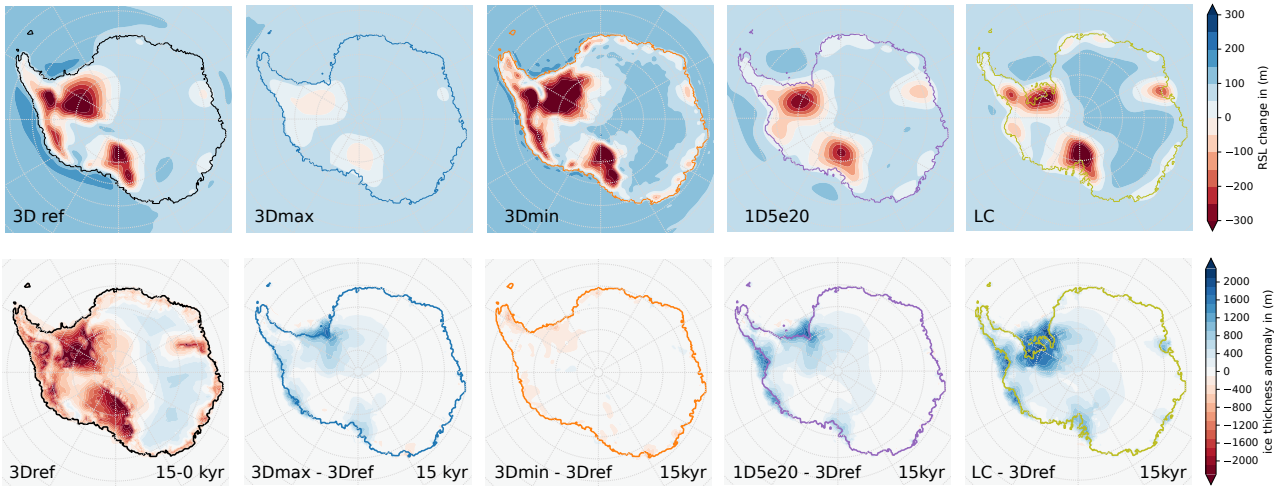

Figure S 3. RSL and ice thickness change since 15 kyr BP, in coupled simulations, for different 3D structures as in Sect. 3.2, and with respect to 1D Earth structure analogous to Lingle-Clark model (LC), as in Sect. 3.3. Corresponding grounding lines at LGM colored. In the lower row, ice thickness anomaly is between LGM (15 kyr BP) and present-day (0 kyr BP) for '3D ref' in the first panel. For the other panels anomaly is between LGM states of different Earth structures.

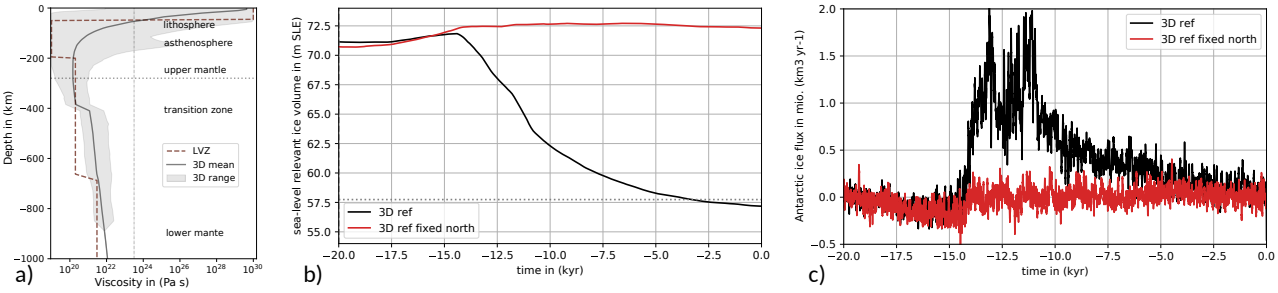

Figure S 4. Global (logarithmic) lateral mean of 3D Earth structures a), sea-level equivalent ice volume b) and ice flux over last 20 kyr c) in experiments with evolving (black) and fixed (red) northern hemisphere deglaciations, analogous to Fig. 2b and Fig. 3a in Gomez et al. (2020). Ice flux, as change in total Antarctic ice volume, has been smoothed with running mean over 100 yr. Red dotted line in a) shows 1D Earth structure ('LVZ') used by Gomez et al. (2020). Vertical line denotes threshold of $> 10^{23.5}$ Pa s defining the lithosphere thickness.

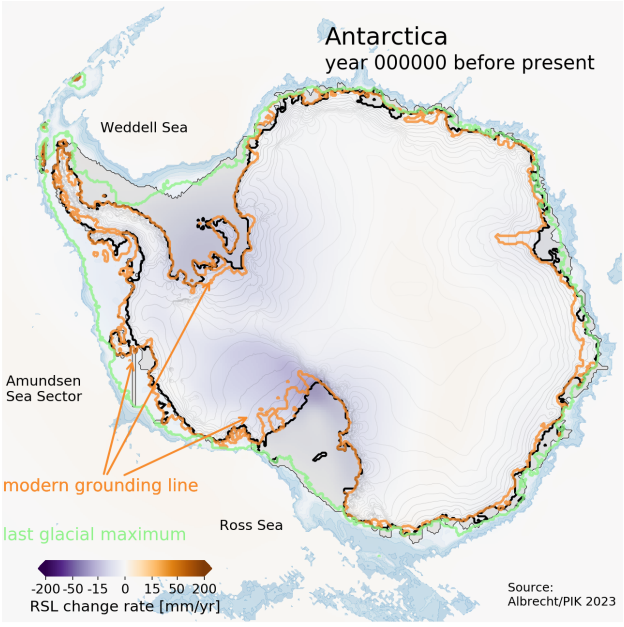

Video S 1: **Change rate of relative sea level (RSL) in Antarctica over the last 25 kyr from a coupled ice sheet–solid Earth model system with reference 3D Earth structure '3D ref'.** Black delineates the grounding line (GL), thin grey the calving front. Green is the GL extent at Last Glacial Maximum, orange the observed present-day GL. Inset shows the global mean sea level change with far-field change rates of up to 50 $\mathrm{mm\,yr^{-1}}$ at around 14.5 $\mathrm{kyr\,BP}$, the Meltwater Pulse 1A. Viscoelastic bedrock uplift in response to marine ice sheet retreat can cause near-field sea level drop of up to -200 $\mathrm{mm\,yr^{-1}}$. Color scale is double logarithmic. Light grey contours indicate ice surface elevation, blue shading indicates the continental shelf up to 1800 m depth. See Video S 1 at: https://doi.org/10.5446/65479

Sensitivity of Antarctic Ice Sheet response to spatial variability in 3D Earth structures

After we have investigated the Antarctic Ice Sheet response coupled to VILMA for the reference 3D Earth structure '3D ref' (v_0.4_s16) compared to high and low viscosity end member 3D structures '3D min' and '3D max', we will now compare the ice sheet response to different 3D structure classes, obtained from the data compilation in Bagge et al. (2020) following their nomenclature. First, we test for another Class-I-type 3D structure '3D glob' (v_1.0_s16), with larger conversion factor (i.e., activation enthalpy factor) between temperature and viscosity and hence larger lateral variability (see range in Fig. S 7a), but also with a higher global log-mean asthenosphere viscosity and a thicker lithosphere. For this Earth structure, VILMA-standalone simulations provide the best fit to a global dataset of present-day uplift rates (Bagge et al., 2023). We also consider the Class-II 3D structure '3D ant' (v_1.0_sc06) with the best fit to a subset of these dataset around Antarctica (36 stations) and with a similar lateral variability, but even higher viscosity in the upper mantle (below $210\,\mathrm{km}$) and lower viscosity in the transition zone at the top of the upper mantle (below $410\,\mathrm{km}$ depth). For comparison, we apply the intermediate Class-III 3D Earth structure '3D trans' (v_1.0_sc06b) with no strong viscosity jump between the upper mantle and the transition zone. All considered 3D Earth structure classes intersect at the top of the transition zone at a depth of $410\,\mathrm{km}$, and converge in the lower mantle below the transition zone (below $670\,\mathrm{km}$).

They can be distinguished by

- the viscosity in the upper mantle and transition zone, determined by the radial viscosity profile
- the lithosphere thickness, determined by the conversion factor and
- the lateral variablity, determined by the conversion factor.

In our coupled simulations, the range of deglacial response of the Antarctic Ice Sheet volume to variation in 3D Earth structure classes is comparably small, with largest differences of about $3\,\mathrm{m\,SLE}$ at LGM (Fig. S 7c) obtained for '3D ref', which also shows the largest sea-level relevant ice volume in Antarctica. Among the considered classes, '3D ref' has the lowest global mean upper-mantle viscosity, the thinnest lithosphere (Fig S 6) and the smallest global range (lateral variability, factor 0.4). For larger lateral variability (factor 1.0) we find for increasing upper mantle viscosity and decreasing lower mantle viscosity (s16, sc06b, sc06, see Fig. S 7a) slightly decreasing ice volumes at LGM. The trajectories of deglacial ice loss over the last $15\,\mathrm{kyr}$ is similar in all classes, converging after $10\,\mathrm{kyr\,BP}$ in the coupled simulations (Fig. S 7c). Already in the first iteration, the three classes with similar lateral variability and lithosphere thickness ('3D glob', '3D trans' and '3D ant') show a very similar ice volume response since LGM, while for '3D ref' the LGM ice volume is larger and the present-day ice volume is smaller (compare transparent lines in Fig. S 7c). Also, the convergence rate for the iterative optimization of present-day bed topography is lowest for '3D ref'. The present-day anomaly is alternating with each iteration and it takes 6 iterations instead of 3 to reach an RMSE below $10\,\mathrm{m}$ (cf. Fig. 4 and Fig. S 7b). Likely, this effect is caused by the thin lithosphere, and is even more pronounced for the lower end '3D min' (Fig. 3c).

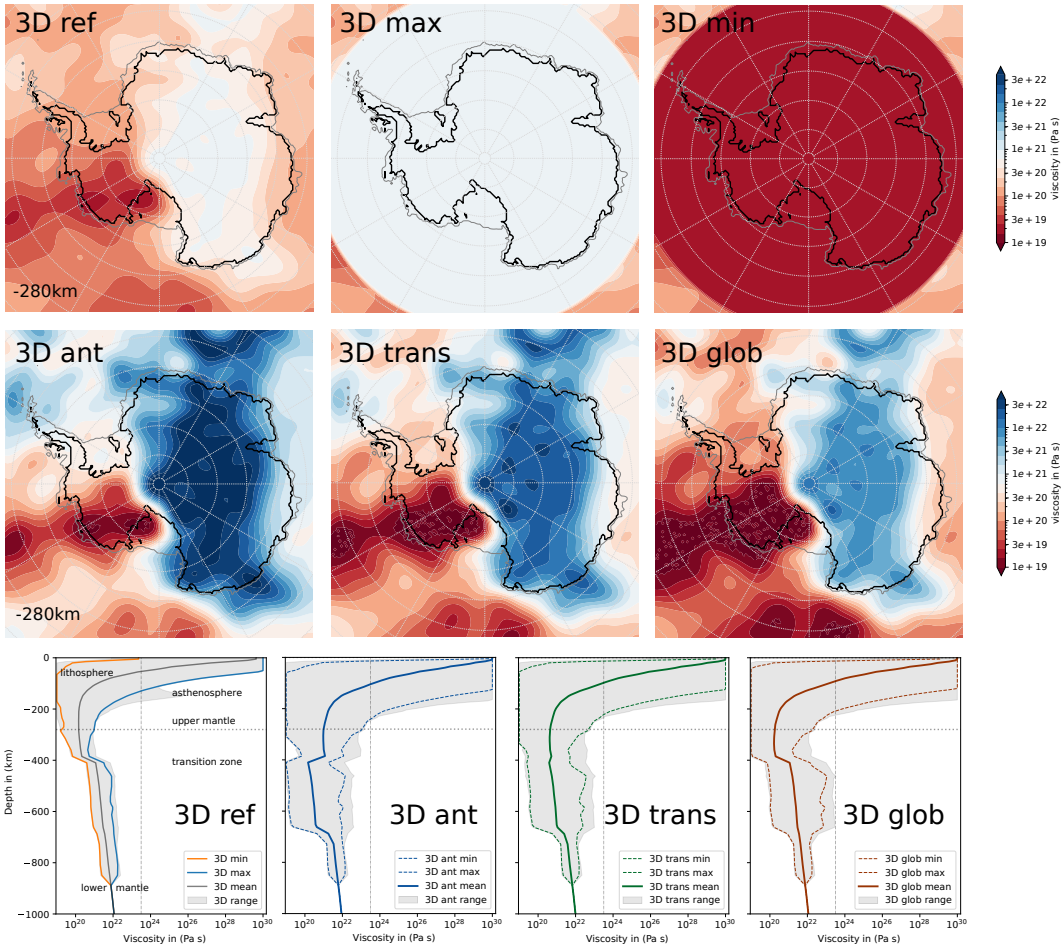

Figure S 5. Earth structures underneath Antarctica with upper-mantle viscosity shown at 280 km depth for the six different 3D structures considered. Vertical profiles show global range, logarithmic mean and minimum and maximum values in Antarctic domain for four of the 3D Earth structures. Note that colorbar range differs from that in Fig. 5b.

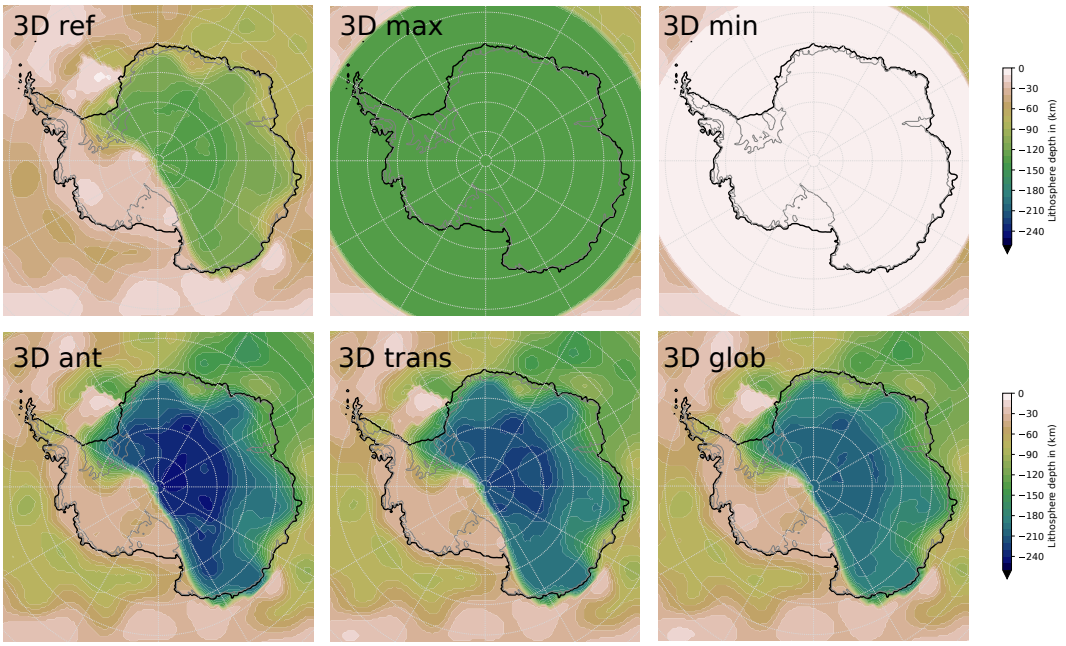

Figure S 6. Lithosphere thickness underneath Antarctica for the six different 3D structures considered. Note that colorbar range differs from Fig. 5c.

In our coupled simulations, the range of deglacial response of the Antarctic Ice Sheet volume to variation in 3D Earth structure classes is comparably small, with largest differences of about 3 m SLE at LGM (Fig. S 7c) obtained for '3D ref', which also shows the largest sea-level relevant ice volume in Antarctica. Among the considered classes, '3D ref' has the lowest global mean upper-mantle viscosity, the thinnest lithosphere (Fig S 6) and the smallest global range (lateral variability, factor 0.4). For larger lateral variability (factor 1.0) we find for increasing upper mantle viscosity and decreasing lower mantle viscosity (s16, sc06b, sc06, see Fig. S 7a) slightly decreasing ice volumes at LGM. The trajectories of deglacial ice loss over the last 15 kyr is similar in all classes, converging after 10 kyr BP in the coupled simulations (Fig. S 7c). Already in the first iteration, the three classes with similar lateral variability and lithosphere thickness ('3D glob', '3D trans' and '3D ant') show a very similar ice volume response since LGM, while for '3D ref' the LGM ice volume is larger and the present-day ice volume is smaller (compare transparent lines in Fig. S 7c). Also, the convergence rate for the iterative optimization of present-day bed topography is lowest for '3D ref'. The present-day anomaly is alternating with each iteration and it takes 6 iterations instead of 3 to reach an RMSE below 10 m (cf. Fig. 4 and Fig. S 7b). Likely, this effect is caused by the thin lithosphere, and is even more pronounced for the lower end '3D min' (Fig. 3c).

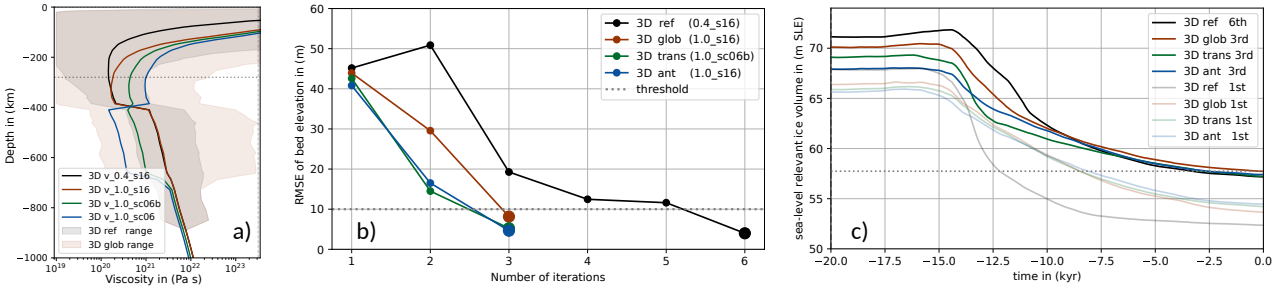

Figure S 7. Global (logarithmic) lateral mean viscosity of 3D Earth structures a), RSL convergence at present b) and corresponding sea level relevant Antarctic ice volume c) over the last 20 kyr for different 3D Earth model configurations. Black color indicates the reference 3D Earth structure '3D ref' (v_0.4_s16, Class-I), red-brown a similar 3D structure but with more lateral variability '3D glob' (v_1.0_s16, Class-I), green an intermediate 3D structure '3D trans' (v_1.0_sc06b, Class-III) and dark-blue the 3D structure that has an opposite viscosity jump between the upper mantle and the transition zone '3D ant' (v_1.0_sc06, Class-II). In a) the range between global mininum and maximum viscosity for '3D ref' is shaded in grey, and redish for the '3D glob' Earth structure with larger lateral variability and thicker lithosphere. In c) for comparison, first iteration results are shown in transparent colors.

References

Bagge, M., Klemann, V., Steinberger, B., Latinovic, M., and Thomas, M.: 3D Earth structures for glacial-isostatic adjustment models, V. 1.0, GFZ Data Services, https://doi.org/10.5880/GFZ.1.3.2020.004, 2020.

Bagge, M., Klemann, V., Steinberger, B., Latinović, M., and Thomas, M.: Glacial-Isostatic Adjustment Models Using Geodynamically Constrained 3D Earth Structures, Geochemistry, Geophysics, Geosystems, 22, e2021GC009 853, https://doi.org/https://doi.org/10.1029/2021GC009853, 2021.

Bagge, M., Boergens, E., Balidakis, K., Klemann, V., and Dobslaw, H.: A validation method for modelled present-day GIA uplift rates against space geodetic data, Solid Earth (in prep.), 2023.

Fretwell, P., Pritchard, H. D., Vaughan, D. G., Bamber, J. L., Barrand, N. E., Bell, R., Bianchi, C., Bingham, R. G., Blankenship, D. D., Casassa, G., Catania, G., Callens, D., Conway, H., Cook, A. J., Corr, H. F. J., Damaske, D., Damm, V., Ferraccioli, F., Forsberg, R., Fujita, S., Gim, Y., Gogineni, P., Griggs, J. A., Hindmarsh, R. C. A., Holmlund, P., Holt, J. W., Jacobel, R. W., Jenkins, A., Jokat, W., Jordan, T., King, E. C., Kohler, J., Krabill, W., Riger-Kusk, M., Langley, K. A., Leitchenkov, G., Leuschen, C., Luyendyk, B. P., Matsuoka, K., Mouginot, J., Nitsche, F. O., Nogi, Y., Nost, O. A., Popov, S. V., Rignot, E., Rippin, D. M., Rivera, A., Roberts, J., Ross, N., Siegert, M. J., Smith, A. M., Steinhage, D., Studinger, M., Sun, B., Tinto, B. K., Welch, B. C., Wilson, D., Young, D. A., Xiangbin, C., and Zirizzotti, A.: Bedmap2: improved ice bed, surface and thickness datasets for Antarctica, The Cryosphere, 7, 375–393, https://doi.org/10.5194/tc-7-375-2013, 2013.

Gomez, N., Weber, M. E., Clark, P. U., Mitrovica, J. X., and Han, H. K.: Antarctic ice dynamics amplified by Northern Hemisphere sea-level forcing, Nature, 587, 600–604, https://doi.org/10.1038/s41586-020-2916-2, 2020.